Archives of Medical Research 52 (2021) 692–702

Hepatic Accumulation of Hypoxanthine: A Link Between Hyperuricemia and Nonalcoholic Fatty Liver Disease

Paola Toledo-Ibelles,[a] Roxana Gutiérrez-Vidal,[b] Sandra Calixto-Tlacomulco,[a] Blanca Delgado-Coello,[a] and Jaime Mas-Oliva[a]

[a] *Departamento de Bioquímica y Biología Estructural, Instituto de Fisiología Celular, Universidad Nacional Autónoma de México. Ciudad de México, México*

[b] *Centro de Investigación y de Estudios Avanzados del Instituto Politécnico Nacional. Unidad Monterrey, Apodaca, Nuevo León, México*

Received for publication December 22, 2020; accepted April 14, 2021 (ARCMED_2020_00120).

Background. An elevated level of plasma uric acid has been widely recognized as a risk factor for non-alcoholic fatty liver disease (NAFLD), where oxidative stress and inflammation play an important role in the pathophysiology of the disease. Although the complete molecular mechanisms involved remain unknown, while under physiological conditions uric acid presents antioxidant properties, hyperuricemia has been linked to oxidative stress, chronic low-grade inflammation, and insulin resistance, basic signs of NAFLD.

Aim of study. Employing *in vivo* experimentation, we aim to investigate whether a high-fat diet rich in cholesterol (HFD), modifies the metabolism of purines in close relationship to molecular events associated with the development of NAFLD. *In vitro* experiments employing HepG2 cells are also carried out to study the phenomenon of oxidative stress.

Methods. Adult male rabbits were fed for 8 weeks an HFD to induce NAFLD. At the beginning of the experiment and every 15 d until the completion of the study, plasma levels of lipids, lipoproteins, and uric acid were measured. Liver tissue was isolated, and histology performed followed by the biochemical determination of hypoxanthine, protein expression of xanthine oxidoreductase (XOR) by western blot analysis, and xanthine oxidase (XO) activity using an enzymatic kinetic assay. Furthermore, we employed i*n vitro* experimentation studying HepG2 cells to measure the effect of hypoxanthine and H_2O_2 upon the production of radical oxygen species (ROS), XO activity, and cell viability.

Results and Conclusion. Hepatic tissue from rabbits fed the HFD diet showed signs of NAFLD associated with an increased ROS concentration and an altered purine metabolism characterized by the increase in hypoxanthine, together with an apparent equilibrium displacement of XOR towards the xanthine dehydrogenase (XDH) isoform of the enzyme. This protein shift visualized by a western blot analysis, associated with an increase in plasma uric acid and hepatocyte hypoxanthine could be understood as a compensatory series of events secondary to the establishment of oxidative stress associated with the chronic establishment of fatty liver disease.

Key Words: NAFLD, NASH, Hypoxanthine, Xanthine oxidoreductase, Xanthine oxidase, Oxidative stress.

Address reprint requests to: Jaime Mas-Oliva, Departamento de Bioquímica y Biología Estructural, Instituto de Fisiología Celular, Universidad Nacional Autónoma de México, Apartado Postal 70-243, 04510 Ciudad de México, México; Phone: (+52) (55) 56225584; FAX: (+52) (55) 56225611; E-mail: jmas@ifc.unam.mx

https://doi.org/10.1016/j.arcmed.2021.04.005

Introduction

According to the World Health Organization, cardiovascular disease (CVD) is the leading worldwide cause of death in the general population (1). This pathology has been extensively associated with multiple factors such as non-alcoholic fatty liver disease (NAFLD), including hepatic steatosis and non-alcoholic steatohepatitis (NASH), known to contribute to the development of cirrhosis and type 2 diabetes (2,3). Several epidemiological studies have shown a positive relationship between the level of uric acid in plasma and the incidence of NAFLD in CVD (4–8), where uric acid has been proposed as a predictor of morbidity and mortality (9–12). Although the relationship between hyperuricemia and NASH may not be a direct one, there is the possibility that both might be associated because of the establishment of metabolic syndrome (13–14).

In the human, the catabolism of purines generates uric acid as an oxidative product of hypoxanthine and xanthine due to the enzyme xanthine oxidoreductase (XOR), mainly expressed in the liver, intestine, and vascular endothelial cells (15). In physiological conditions, this enzyme presents two interconvertible forms by a disulfide bond formation. The first one corresponds to xanthine dehydrogenase (XDH), the most common isoform found in cells, that uses NAD^+ as an electron acceptor to produce NADH. While xanthine oxidase (XO) transfers electrons directly to molecular oxygen with the concomitant generation of reactive oxygen species (ROS) and particularly H_2O_2, and therefore, considered an essential source of reactive peroxides, superoxide, hydroxyl radical, singlet oxygen, and α-oxygen (16,17). While to date oxidative stress is a key factor in the development of NASH and CVD (18), in the hepatocyte, the molecular mechanisms that correlate the metabolism of purines with a state of oxidative stress following a lipid overload, are still a matter of intensive study. Although uric acid is a risk factor for fatty liver disease and CVD (14,19), the molecular mechanisms involved in the way hepatocytes respond to uric acid also remain to be studied, together with the question if oxidative stress potentiates the effects of hyperuricemia.

Our data indicate that liver cells from experimental animals fed a high cholesterol/triglyceride diet show an increase in hypoxanthine that promotes an equilibrium displacement of XOR activity towards the XDH form of the enzyme. This phenomenon is most probably associated with the process of activation/inactivation of diverse enzymes involved in the proteolysis of XDH, under an increased hypoxanthine concentration. Considering that it has been shown that under acute cellular oxidative conditions the proteolytic induction of XO is favored, the compensatory mechanisms activated during established chronic metabolic conditions are still a matter of controversy. Therefore, we believe the study of this enzyme in the hepatocyte under conditions of oxidative stress and hypoxanthine accumulation associated with fatty liver disease acquires special relevance in the understanding of how NAFLD and NASH are established as important participants of CVD.

Methods

Experimental Animal Procedures

All animal procedures were performed following the Guide for the Care and Use of Laboratory Animals (NIH), and approved by the Animal Ethics Committee, Instituto de Fisiología Celular, Universidad Nacional Autónoma de México (protocol JMO90-16). Male New Zealand white rabbits ($n=6$) weighing between 2.2–2.9 kg was divided into two groups.

Animals were housed at 20°C on a 12:12 h light/dark cycle, fed *ad libitum*, and allowed free access to water. Rabbits from the control group (CT) ($n=3$) were fed a standard diet (Laboratory Rabbit Diet, Brentwood, MO, USA). The second group was fed a high-fat diet (HFD) ($n=3$) composed of the standard diet supplemented with 10% corn oil and 1% cholesterol (Sigma-Aldrich, St. Louis MO, USA). At the beginning of the experiment and every 2 weeks, blood was collected from the marginal ear vein after 14 h of overnight fasting. At the end of the study on an anesthetized animal, blood was obtained by cardiac puncture. Serum and plasma-EDTA samples were used for biochemical and enzymatic measurements using standardized methods, and carried out at Departamento de Patología, Facultad de Veterinaria y Zootecnia, Universidad Nacional Autónoma de México. Employing the same experimental animal model and a similar dietary regime that we use in the present study; pathological signs of well-defined fatty liver disease have been identified by us in both the rabbit and the pig (20–23).

Histological Analysis

At the time of euthanasia, liver samples from the right lobe were collected and a portion of these samples fixed in 10% formaldehyde. Samples were embedded in paraffin and stained with classical hematoxylin-eosin (H&E) to study cell morphology and Masson's trichrome stain that highlights the deposition of collagen fibers characteristic of fibrosis. The remaining tissue was frozen in liquid nitrogen and stored at –80°C until further analysis. Liver sections were evaluated considering histopathological characteristics for NAFLD: steatosis, inflammation, ballooning, and the presence of fibrosis (24). Preparations were analyzed using conventional light microscopy and multiphoton microscopy. Briefly, multiphoton microscopy images from all liver samples were acquired using water immersion objectives: C-Apochromat 10x and W Plan-Apochromat 20x, with a 40x optical zoom. Second-harmonic generation

analysis was performed using a galvanometer-based scanning system LSM 710Zeiss and a Ti: sapphire laser (coherent) employing a wavelength of 900 nm wavelength (12% of laser power) and a BP 420–480 nm filter (Zeiss).

Hypoxanthine and Xanthine Oxidase Activity Measurements

Hypoxanthine levels and XO activity in hepatic tissue were measured with the Amplex Red Xanthine/Xanthine Oxidase Assay kit (Thermo Fisher Scientific, Waltham, MA, USA). This kit provides a sensitive method for detecting xanthine/hypoxanthine, or for monitoring xanthine oxidase activity in the supernatant of homogenized liver tissue samples. Hepatic tissue is homogenized employing saline cold buffer and clarified by centrifugation. A further dilution of the supernatant with the reaction buffer is employed to determine the endpoint fluorescent signal. In the assay, xanthine oxidase catalyzes the oxidation of xanthine/hypoxanthine, to uric acid and superoxide (H_2O_2), and the H_2O_2 in the presence of horseradish peroxidase reacts stoichiometrically with the Amplex Red reagent to generate the red-fluorescent oxidation product, resorufin. This compound presents absorption and fluorescence emission maxima of approximately 571 nm and 585, respectively. On the other hand, intracellular hypoxanthine concentrations and XO activity of HepG2 cells were measured with kits from Ray Biotech (Norcross, GA, USA), and Abcam (Cambridge, MA, USA), respectively. The RayBio xanthine/hypoxanthine assay employs a xanthine enzyme mix that specifically oxidizes xanthine/hypoxanthine to form an intermediate, which reacts with Developer and Probe to form a product that can be measured fluorometrically with absorption and fluorescence maxima at 525/587 nm. The Abcam xanthine oxidase activity assay also employs the oxidation of xanthine/hypoxanthine to H_2O_2 which reacts stoichiometrically with a probe to generate fluorescence showing an absorption and fluorescence maxima at 535/587 nm. With both kits, standard curves are prepared according to the manufacturer's instructions and employed in the determination of values from experimental samples. Independently of the kit employed, after different treatments had taken place, culture medium was removed from Petri dishes, and cell monolayers washed three times with PBS at room temperature. Immediately after, cells are detached by using trypsin incubating for 5 min at 37°C, followed by trypsin inactivation using FBS supplemented DMEM, cells are washed once more, centrifuged, and supernatants discarded. For the determination of hypoxanthine concentration and XO activity, the number of cells employed are first standardized, to be further lyzed, clarified by centrifugation, and supernatants used for both measurements.

Xdh Gene Expression by qPCR

Total liver RNA was isolated with Trizol reagent (Thermo Fisher Scientific); 1μg was used to synthesize cDNA using the iScript cDNA synthesis kit (Bio-Rad). The expression of *xanthine dehydrogenase* (*XDH:* 5'-CCATCTACGCTTCCAAGGCT-3' and 5'-CAGTGACACACAGGGTGGTGA-3') and *glyceraldehyde dehydrogenase* (*GAPDH*: 5'-TCGGAGTGAACGGATTTGGC-3' and 5'-CCAGCATCACCCCACTTGAT-3') transcripts were determined by qPCR using the PowerUp Sybr Green Master Mix 2X (Applied Biosystems, CA, USA) on an ABI PRISM 7000 Sequence Detection cycler. All samples were analyzed in triplicates and the results are relative levels of mRNA calculated as $2^{-\Delta\Delta Ct}$.

XOR Protein Expression by Western Blot Analysis

Liver samples were homogenized in cold RIPA buffer (Thermo Fisher Scientific) supplemented with protease inhibitors (Roche). Protein concentration was determined using the DC Protein Assay (Bio-Rad, CA, USA), and 100 μg of liver lysates were separated in 8 or 10% polyacrylamide gels (SDS-PAGE) and transferred to PVDF membranes (MilliporeMerck, Burlington, MA, USA). Blots were incubated with specific antibodies from Santa Cruz Biotechnology (Santa Cruz, CA, USA) recognizing XOR (XDH/XO) (sc-398548) and GAPDH (sc-47724).

Cell Culture

HepG2 cells (ATCC HB-8065) were grown following ATCC instructions, employing Dulbecco's Modified Eagle Medium (DMEM) (Thermo Fisher Scientific) supplemented with 10% fetal bovine serum, 10 μg/mL streptomycin, 0.25 μg/mL amphotericin, and 100 U/mL penicillin at 37°C and 5% CO_2. Usually after 72 h of incubation with cells reaching 80–90% confluency, cells are rinsed with PBS and exposed to 80 mmol H_2O_2 diluted in DMEM. After 1h exposure, cells were trypsinized and reseeded in a proportion of 4.6×10^4 cells/cm^2 in DMEM supplemented medium, with the addition of hypoxanthine from a 1M stock solution solubilized in NaOH. Final concentrations ranged from 25–150 mmol hypoxanthine and 156 mmol NaOH, for all conditions including negative controls. Under these conditions, no significant changes on medium pH were observed. When indicated, allopurinol 10 mmol (25), methionine 25 or 50 mmol (26), or Trolox at 25 or 50 μM (27), were added to DMEM, and cells incubated in this medium for 12 h before the oxidative stimulus with H_2O_2 (28), and exposure to hypoxanthine takes place.

Cell Viability

The integrity of the plasma membrane was used as a marker of cell viability, measuring lactic dehydrogenase activity released to the medium. In lysates, results were expressed as a percentage of lactic dehydrogenase activity released to the medium (29). Collected samples were incubated for 5 min in a Tris/NaCl buffer (pH 7.2) with NADH 0.3 mmol, on 96 well plates for UV spectrophotometric readings to follow NADH consumption. The reaction was initiated by adding sodium pyruvate (10 mmol, final concentration) and performed at 30°C. Immediately after starting the reaction, absorbance at 340 nm was measured and changes registered every 30 s for 5 min.

Intracellular Reactive Oxygen Species

Cells grown in 96 well plates, at the different study conditions, supplemented and washed with PBS at 37°C were further incubated for 45 min in DMEM and 10 mmol dichlorofluorescein diacetate. Cell suspensions were obtained and transferred to a 96 well dark plate to measure fluorescence at 485/528 nm (excitation/emission). Results were expressed as the percentage of ROS with respect to confluent cells in the absence of the stimulus.

Statistical Analysis

Data are expressed as mean ± SEM. Statistical significance was determined by a two-tailed Student's *t*-test or *U* Mann Whitney, depending on variables' distribution; $p < 0.05$ was considered statistically significant ($^{*}p < 0.05$). Analysis of the data was performed with the SPSS v20 program (Chicago, USA).

Results

Hepatic Tissue Examination

At the end of the 60 d of the experiment, animals were sacrificed, and liver samples prepared from both experimental groups (control and HFD). To ensure that tissue damage associated with NAFLD had been established, samples were examined by conventional light microscopy and second-harmonic generation microscopy. Figure 1 shows representative images of samples belonging to each one of the two experimental groups studied, displaying the central vein surrounded by layers of hepatocytes. In contrast to rabbits fed the standard diet showing a normal tissue structure and a normal collagen distribution (Figure 1A, C), rabbits fed an HFD show microvesicular steatosis, cellular ballooning, and inflammation, as characteristic signs of NASH (Figure 1B). Moreover, using Masson's trichrome stain, it was possible to visualize the presence of extensive collagen fiber deposition, denoting the presence of fibrosis and progressive hepatic disease (Figure 1D). The use of second-harmonic generation microscopy, useful in the evaluation of tissue areas with increased deposition of protein shows an extensive network of collagen fibril/fiber structures, supporting the fibrotic feature of livers in the HFD experimental group (Figure 1E, F).

Plasma Metabolite Profiles

To address whether the metabolism of lipid and purines are simultaneously altered during the process of NASH consolidation, the following plasma parameters were measured at the start of the experiment and every two weeks before sacrifice; total cholesterol, triglycerides, C-LDL, C-HDL, and uric acid. As expected, values for lipids such as total cholesterol, triglycerides and C-LDL were increased by the HFD (Figure 2A-C), while the C-HDL levels were to remain close to values observed with control animals (Figure 2D). Interestingly, immediately after the start of the HFD, plasma levels for uric acid dramatically increased in correlation to the plasma levels of cholesterol (Figure 2E).

Hypoxanthine and XOR in NASH

In contrast to the control group, the plasma concentration of hypoxanthine in the HFD group showed a significant elevation (Figure 3A). Surprisingly, XO activity that did not show changes between groups fed or not with the HFD (Figure 3B), also, did not present differences in transcript expression of *Xdh* (Figure 3C).

Nevertheless, a western blot analysis using an anti-XOR antibody that recognizes both isoforms of the enzyme (XDH and XO), shows that liver lysates from control animals present two bands very close to each other at the expected molecular weight region for XOR, a result that most probably corresponds to the presence of the two enzyme isoforms. An upper band containing the molecular form XDH, and a lower molecular weight band reported to be exclusively associated with XO, and normally related to changes in the oxido/reduction equilibrium of cysteines 535 and 992. Although under normal conditions this equilibrium is maintained, it is found that under an adverse cell metabolic condition due to an HFD, a potential oxidative environment promotes an equilibrium shift towards the XDH form of the enzyme (Figure 3D).

Hypoxanthine Effect on Hepatocytes

To further explore if the increase in cell hypoxanthine established in the HFD group is associated to an oxidative environment, we performed a series of *in vitro* experiments employing 72 h hypoxanthine treated HepG2 cells. Under these conditions, we found the concomitant increase in intracellular hypoxanthine associated to an increment in XO activity (Figure 4A). When the concentration of hypoxanthine is increased up to 125 mmol, treated cells show a

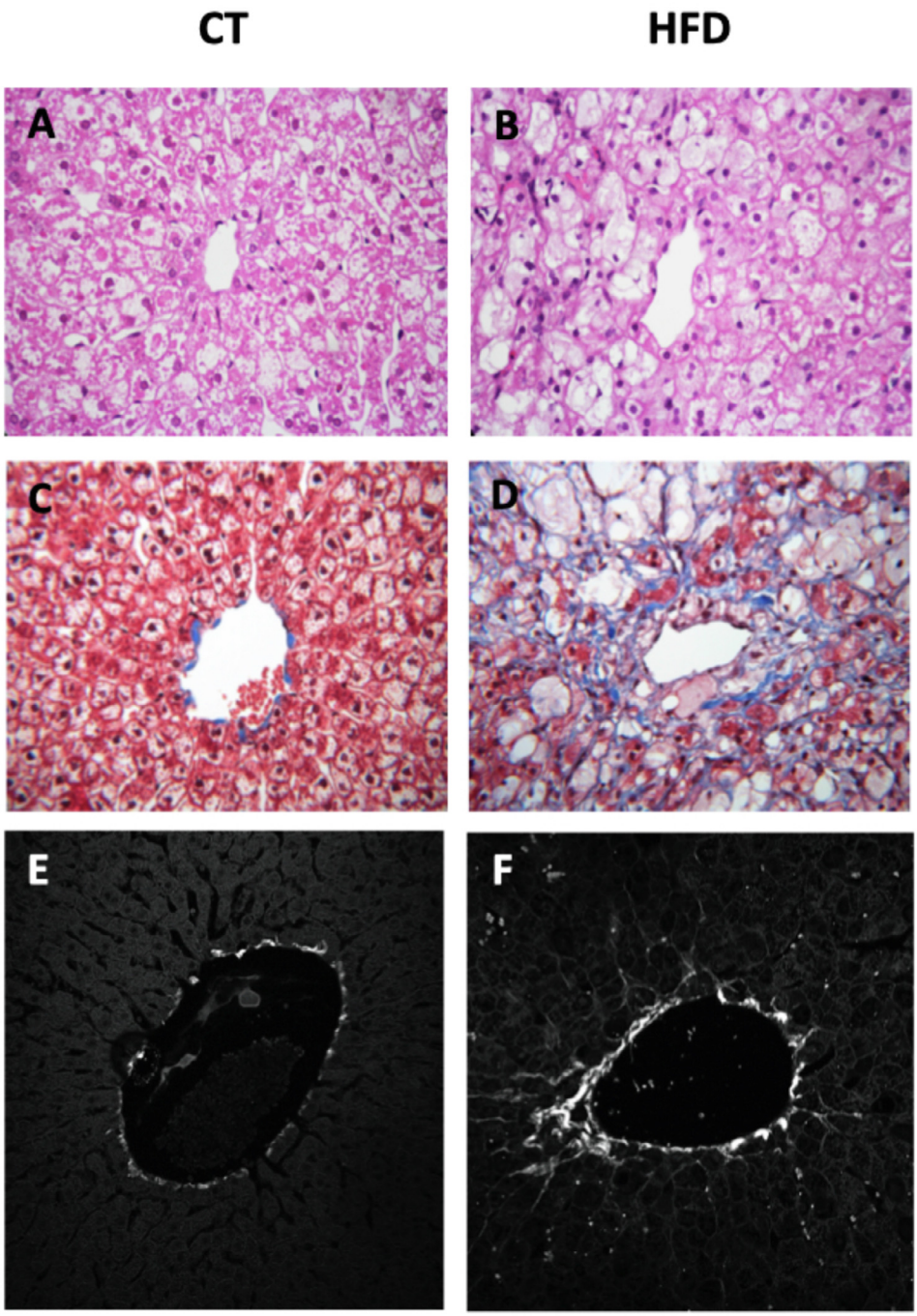

Figure 1. The high-fat diet induces NAFLD in rabbits. Representative images showing the central vein surrounded by hepatocytes of a representative rabbit from each experimental group. (A,C,E) Images from hepatic tissue from the control group fed a normal diet. (B,D,F) Hepatic tissue from animals fed the HFD. (A,B) Hematoxylin-eosin stain (light microscopy). (C,D) Masson's trichrome stain (light microscopy). (E,F) Multiphotonic microscopy with second-harmonic generation images.

marked ROS production, with no apparent affectation in cell viability up to 100 mmol (Figure 4B). Since during these experiments designed to have acute exposure and response to hypoxanthine, a rise in XO activity has been established, and the potential generation of H_2O_2 might be occurring, HepG2 cells were also treated with increasing concentrations of H_2O_2. Under these conditions, a further increase in the intracellular concentration of ROS was observed, associated with a negligible impact on cell viability, again up to 100 mmol (Figure 4C).

To further explore if hypoxanthine by itself contributes to the state of oxidative stress, HepG2 cells

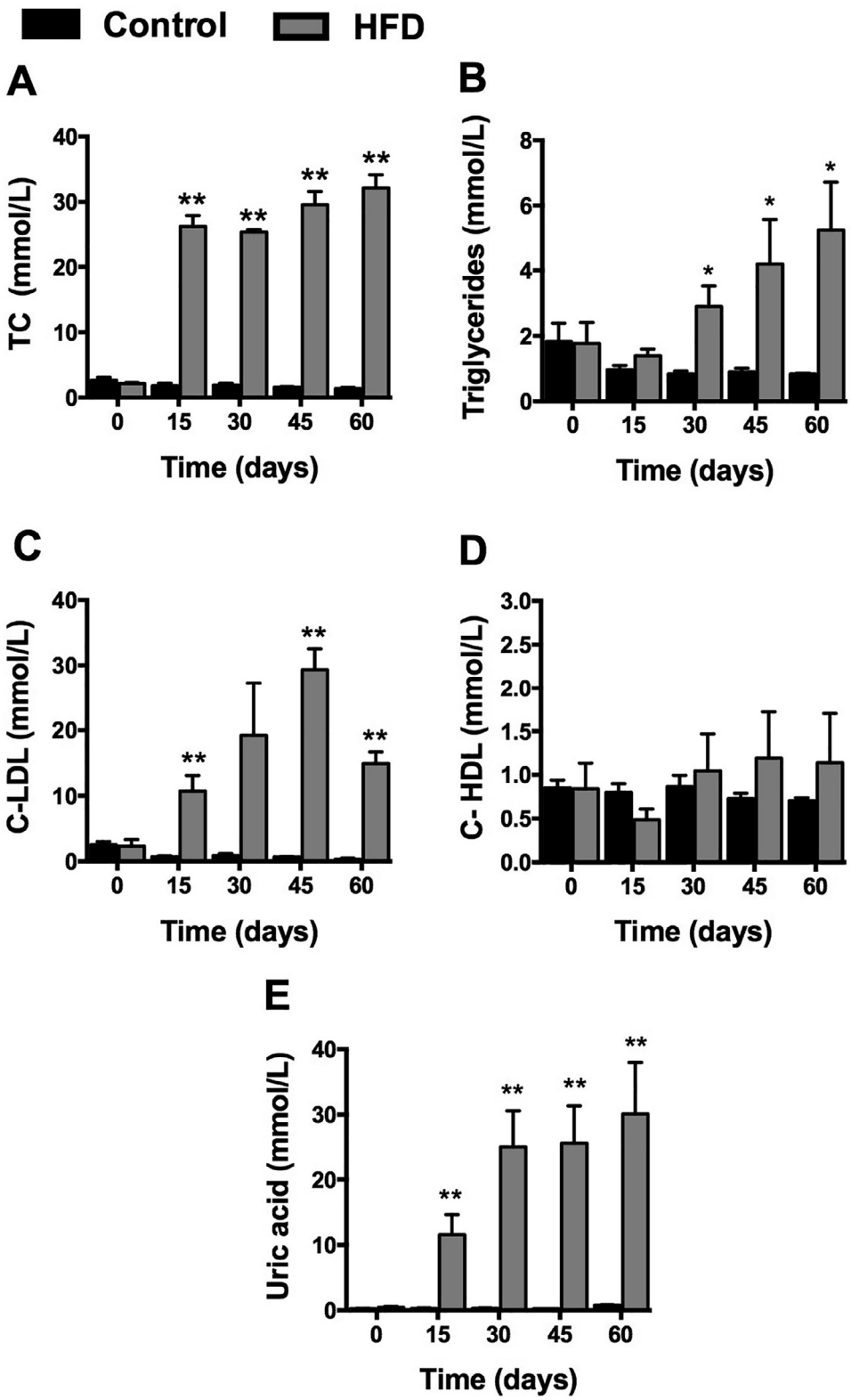

Figure 2. Biochemical parameters in plasma. Plasma samples from rabbits fed a standard diet (CT, $n=3$) or a high-fat diet that include cholesterol (HFD, $n=3$) were analyzed for: (A) Total cholesterol; (B) Triglycerides. (C) C-LDL; (D) C-HDL. (E) Uric acid. ($^{*}p < 0.05$; $^{**}p < 0.01$).

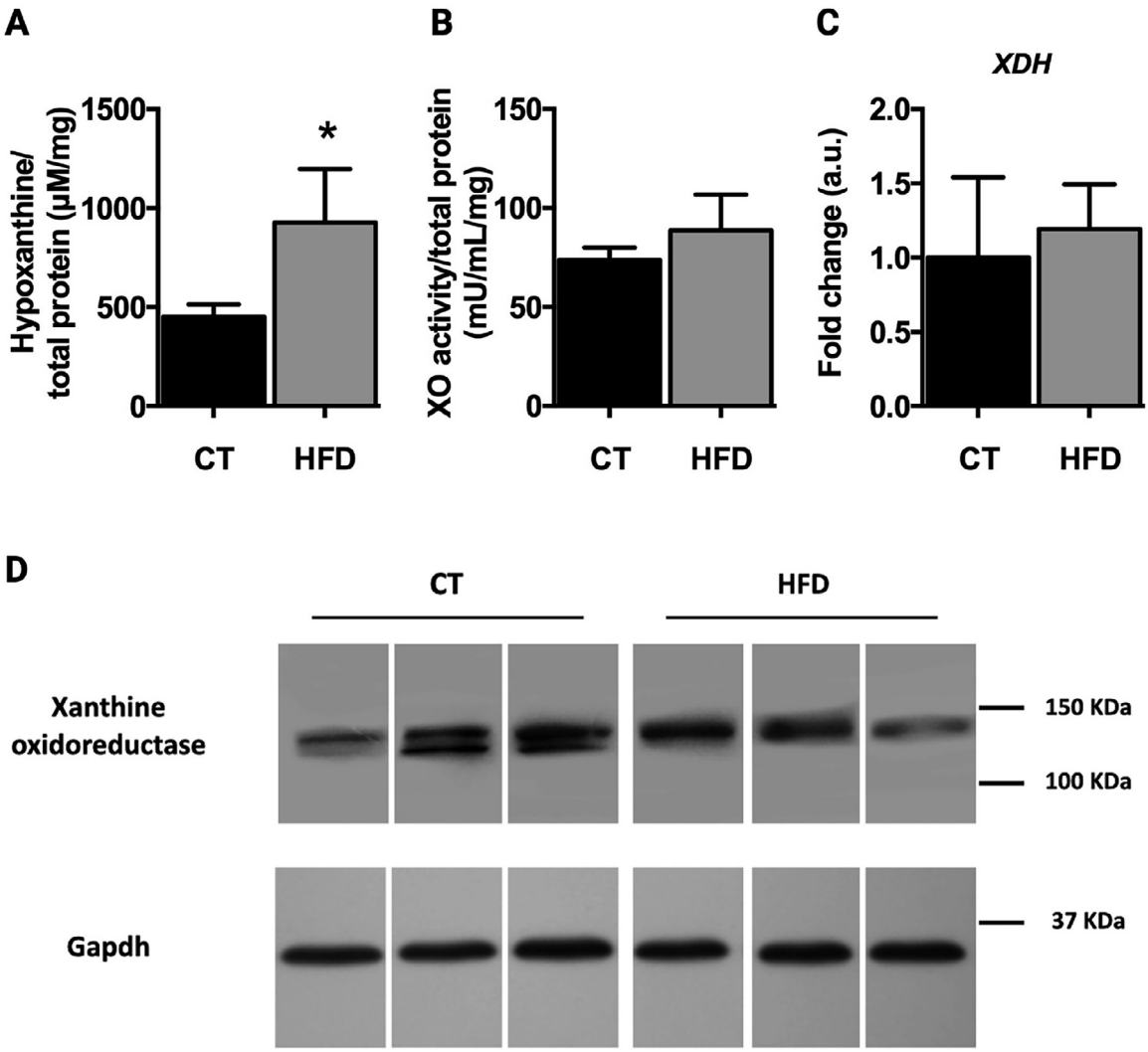

Figure 3. Analysis of purine metabolites and XO activity in liver lysates. (A) Hypoxanthine ($n=5$); (B) XO activity ($n=5$). (C) *XDH* transcripts ($n=5$) ($^{*}p$ <0.05). (D) Western blot analysis of XDH/XO. Samples from the three experimental animals fed a standard diet (CT), or a high-fat diet (HFD).

were incubated with the XO inhibitor allopurinol (25) before treatment with 50 mmol hypoxanthine. Under these experimental conditions, oxidative stress was reduced by allopurinol, showing ROS values similar to levels found in control cell cultures (Figure 4D).

Furthermore, the addition of Trolox (25 mmol) a water-soluble antioxidant molecule analog of vitamin E (27), and methionine known to have an antioxidant effect through induction of the antioxidant protein heme oxygenase-1 (26), prevented the induction of oxidative stress derived from cell exposure to hypoxanthine (Figure 4E).

Discussion

Nowadays it has been well established that a high-fat diet that includes cholesterol induces hyperlipidemia associated with metabolic complications such as NASH, hyperglycemia, insulin resistance, dyslipidemia, and even metabolic syndrome (30). Our study shows that such a diet leads to a significant elevation of plasma triglycerides and cholesterol, simultaneously increasing the concentration of uric acid, suggesting that hyperlipidemia alters the metabolism of purines together with the development of liver steatosis and fibrosis as described in NASH (31).

Hyperuricemia as a common condition in patients with fatty liver disease and other metabolic complications, is currently considered as a biomarker of metabolic dysfunction (32), consistent with the observation that the metabolism of purines is modified by an increased lipid content of cells in association with steatohepatitis (33). The present study employing a NAFLD model developed in the rabbit identifies a high plasma uric acid concentration and an increased level of hypoxanthine in the liver, associated to the development of a state of oxidative stress that seems to affect the equilibrium between XDH and XO, as the two catalytic forms of XOR (Figure 5). Since

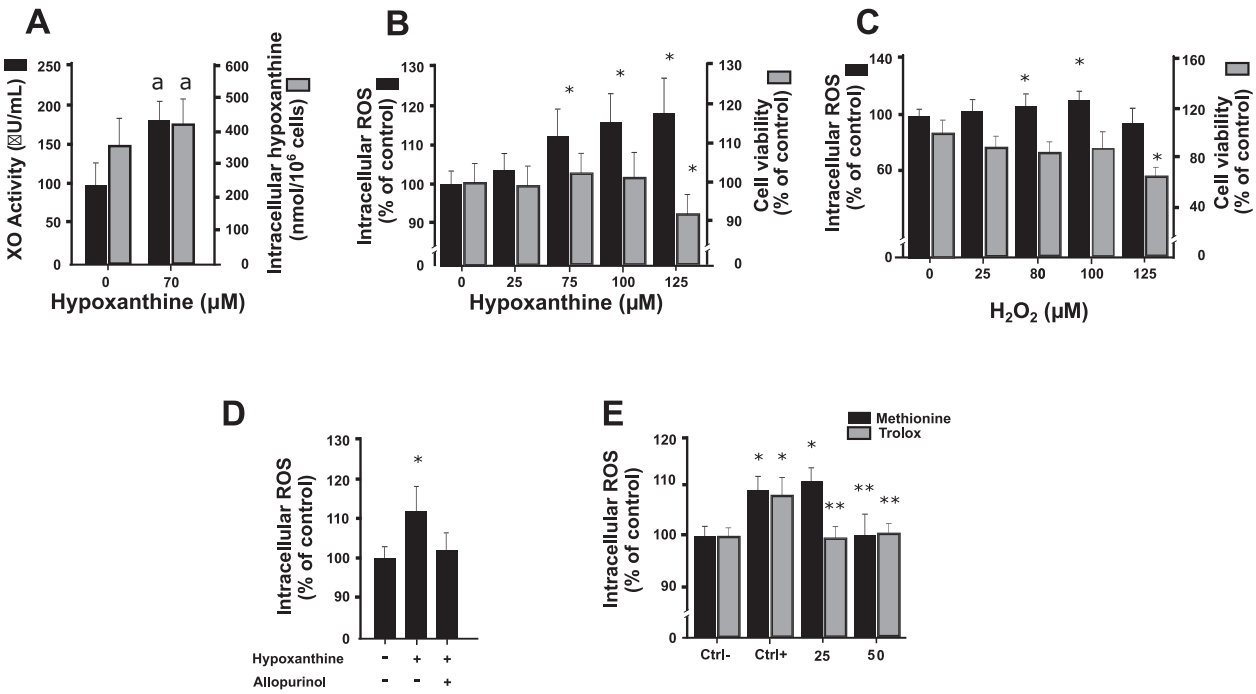

Figure 4. Hypoxanthine effect upon oxidative stress employing HepG2 cells. Cells were grown for 72 h in the presence of hypoxanthine and the following parameters measured. (A) XO activity and corresponding cell viability ($n=5$). (B) Intracellular ROS concentration and cell viability ($n=5$). (C) Intracellular ROS concentration and viability of cells exposed to H_2O_2 ($n=5$). (D) Intracellular ROS concentration in HepG2 cells incubated with 10 mmol allopurinol and 50 mmol hypoxanthine ($n=5$). (E) Intracellular ROS concentration of cells incubated with Trolox and methionine (25 mmol and 50 mmol) ($n=5$). In all experiments, samples were compared against negative controls employing the Student's *t*-test (^{a}p <0.05), except in (E) compared with positive control as well. Significance was defined as $^{*}p$ <0.05 vs. negative control and $^{**}p$ <0.01 vs. positive control.

endothelial cells have shown such an activity transition for XOR induced by H_2O_2 and calcium (18), we shall have to further investigate if in the hepatocyte, associated to oxidative stress, the intracellular concentration of calcium might also present such a modulatory role. This could be particularly important, since it is well known that calcium regulates the activity of a series of proteolytic enzymes (34–36) that might affect not only the catabolism of lipids, but also the catabolism of nucleotides.

Since rabbits soon after the start of the hyperlipidemic diet show signs of development of an oxidative stress state, the study of new metabolic pathways thought out as compensatory mechanisms to counteract the presence of a highly oxidative environment, become important to be investigated (37). Studies performed with patients showing a well-established process of fatty liver disease and atherosclerosis, present an increase in plasma uric acid, considered to be an antioxidant molecule (38). It has been also established, that the catabolism of purines is accelerated before zygote genomic activation, when the activation of transcription by the embryonic genome and the destruction of much of the pre-existing maternal mRNA takes place (39). At this time, secondary to the generation of ROS, the enzyme hypoxanthine/guanine phosphoribosyltransferase (HGPRT), well known to be implicated in salvaging purines, apparently becomes inhibited allowing the cell concentration of hypoxanthine to increase (40).

Supported by these findings, under our experimental conditions, we believe the increase in plasma uric acid, and cellular hypoxanthine, in association to the equilibrium displacement between XDH and XO might be working in parallel as part of a series of compensatory mechanisms triggered in response to a highly oxidative environment found in the hepatocyte because of lipid overload (Figure 5). Moreover, it is interesting to mention that experimentation employing HepG2 cells in culture has shown that uric acid induces the accumulation of lipids (41). This accumulation of lipids dependent upon the intracellular concentration of hypoxanthine and uric acid, and the presence of oxidative stress associated with the establishment of fatty liver disease, seem to contribute to set the stage for the development of fibrosis and eventually to cirrhosis (15,42). On the other hand, while the excretion of uric acid from the hepatocyte is carried out through a concentration-dependent mechanism by urate transporters (UAT), mainly OAT3 (43), an increased intracellular concentration of uric acid activates the enzyme nicotinamide adenine dinucleotide phosphate oxidase (NOX) in cell membranes, producing endoplasmic reticulum stress and further ROS production (44).

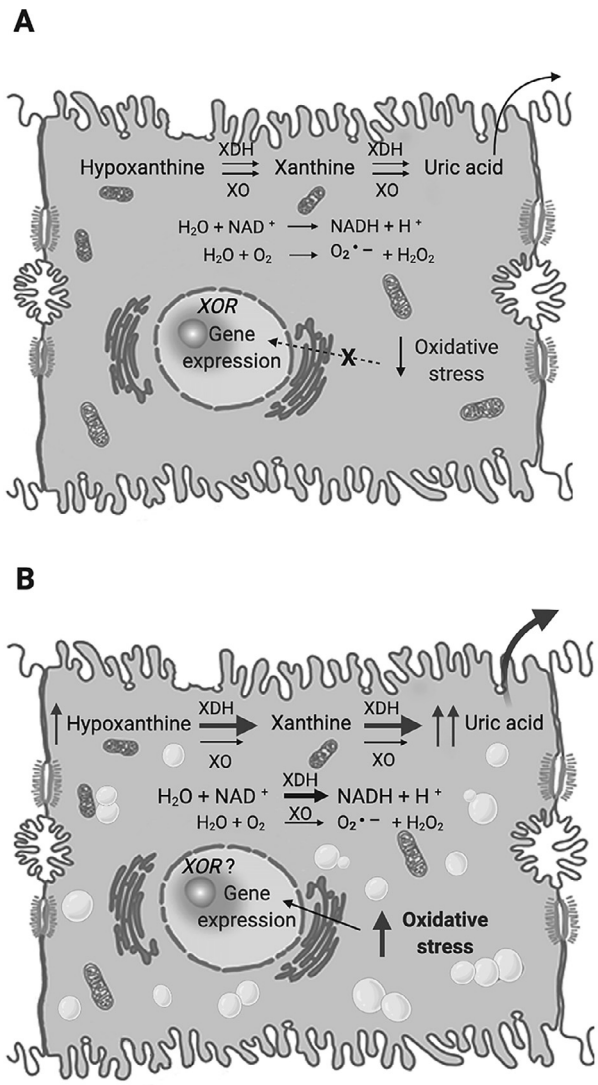

Figure 5. Schematic diagram of the hepatocyte main molecular changes involved in the equilibrium displacement between the molecular forms of XOR under a well-established lipid overload. (A) Normal hepatocyte. (B) Diseased hepatocyte showing oxidative stress and NASH features. Arrows in red show the increase in hypoxanthine, the final pathway molecule uric acid, and the presence of an important oxidative environment. Under our experimental conditions, although lipid overload and oxidative stress apparently did not affect *XDH* transcripts, and the equilibrium changes observed between XDH and XO might be exclusively explained by post-translational modifications, the possibility to have gene expression changes must be further explored.

In contrast to the *in vivo* results employing liver tissue, *in vitro* experimentation employing HepG2 cells cultured under a state of acute oxidative stress, show an increased XO activity. These results support the possibility that cells during a short exposure to an oxidative environment, maintain a high XO activity contributing to set the well-stablished state of oxidative stress. In support of this possibility, cell cultures exposed to a high concentration of lipids or fructose have been shown to importantly increase the intracellular concentration of ROS (45). Moreover, studies using HepG2 cells clearly show H_2O_2 as a source of oxidative stress (46). These results support the fact that in our study, H_2O_2 treated cells contribute to the state of oxidative stress above basal values given by the formation of intracellular ROS.

For some time, it has been known that during specific metabolic states associated with elevated oxidative stress, the metabolism of lipids can be modulated through changes in protein expression in such a way that the balance for key proteins can be affected contributing to the development of fatty liver disease and atherosclerosis (47,48). Since as shown by our group, the generation of oxidative stress has been also linked with gene processing as well as protein expression (49,50), the present study supports the possibility that regulation of nucleotide catabolism in the hepatocyte, might also contribute to modulate the deleterious effects of lipid accumulation in fatty liver disease. Therefore, it will be of special interest employing conditions similar to the ones used in the present study, to directly assay not only XDH and XO activities, but also HGPRT, and seek the specific molecular mechanisms behind the regulation of these enzymes in the hepatocyte during a state of oxidative stress, in an attempt to better understand the development of fatty liver disease associated with CVD.

Conflict of Interest

The authors declare no conflict of interest.

Acknowledgments

This work was supported by grants from DGAPA, UNAM (IN-205717; IN-206619), and CONACYT (255778) awarded to J. Mas-Oliva. P. Toledo-Ibelles is a PhD. student, and S. Calixto-Tlacomulco an M. Phil. student of Programa de Posgrado en Ciencias Bioquímicas, Universidad Nacional Autónoma de México. Both students have received a scholarship from CONACyT for the development of their graduate program. We thank Santa Cruz Biotechnology for the donation of the anti-xanthine oxidase monoclonal antibody employed in this study. We also thank members of the Molecular Biology Unit at IFC-UNAM, Héctor Malagón for expert animal handling, and Jorge Bravo-Martínez for valuable discussions and graphical art support.

References

1. The World Health Organization. Hearts. Technical Package for Cardiovascular Disease Management in Primary Health Care (2016) ISBN 978 92 4 151137. Available at: www.who.int/cardiovascular_diseases/hearts/Hearts_package.pdf.
2. Buzzetti E, Pinzani M, Tsochatzis EA. The multiple-hit pathogenesis of non-alcoholic fatty liver disease (NAFLD). Metabolism 2016;65:1038–1048. doi:10.1016/j.metabol.2015.12.012.

3. Gupte P, Amaraúrkar D, Agal S, et al. Non-alcoholic steatohepatitis in type 2 diabetes mellitus. J Gastroenterology Hepat 2004;19:854–858. doi:10.1111/j.1440-1746.2004.03312.x.
4. Kohn P, Prozan G. Hyperuricemia; relationship to hypercholesterolemia and acute myocardial infarction. JAMA 1959;170:1909–1912. doi:10.1001/jama.1959.03010160025007.
5. Martínez-Quintana E, Tugores A, Rodríguez-González F. Serum uric acid levels and cardiovascular disease: The Gordian knot. J Thorac Dis 2016;8:E1462–E1466. doi:10.21037/jtd.2016.11.39.
6. Zhou Y, Wei F, Fan Y. High serum uric acid and risk of nonalcoholic fatty liver disease: A systematic review and meta-analysis. Clin Biochem 2016;49:636–642. doi:10.1016/j.clinbiochem.2015.12.010.
7. Culleton BF, Larson MG, Kannel WB, et al. Serum uric acid and risk for cardiovascular disease and death: The Framingham Heart Study. Ann Intern Med 1999;131:7–13. doi:10.7326/0003-4819-131-1-199907060-00003.
8. Lonardo A, Bellentani S, Argo CK, et al. Epidemiological modifiers of non-alcoholic fatty liver disease: Focus on high-risk groups. Dig Liver Dis 2015;47:997–1006. doi:10.1016/j.dld.2015.08.004.
9. Madsen TE, Muhlestein JB, Carlquist JF, et al. Serum uric acid independently predicts mortality in patients with significant angiographically defined coronary disease. Am J Nephrol 2005;25:45–49. doi:10.1159/000084085.
10. Wang R, Song Y, Yan Y, et al. Elevated serum uric acid and risk of cardiovascular or all-cause mortality in people with suspected or definite coronary artery disease: A metaanalysis. Atherosclerosis 2016;254:193–199. doi:10.1016/j.atherosclerosis.2016.10.006.
11. Silbernagel G, Hoffmann MM, Grammer TB, et al. Uric acid is predictive of cardiovascular mortality and sudden cardiac death in subjects referred for coronary angiography. Nutr Metab Cardiovasc Dis 2013;23:46–52. doi:10.1016/j.numecd.2011.02.008.
12. Fang J, Alderman MH. Serum uric acid and cardiovascular mortality the NHANES I epidemiologic follow-up study, 1971-1992. National Health and Nutrition Examination Survey. JAMA 2000;283:2404–2410. doi:10.1001/jama.283.18.2404.
13. Batelli MG, Bartolotti M, Polito L, et al. The role of xanthine oxidoreductase and uric acid in metabolic syndrome. Biochim Biophys Acta Mol Basis Dis 2018;1864:2557–2565. doi:10.1016/j.bbadis.2018.05.003.
14. Kushiyama A, Nakatsu Y, Matsunaga Y, et al. Role of uric acid metabolism-related inflammation in the pathogenesis of metabolic syndrome components such as atherosclerosis and nonalcoholic steatohepatitis. Mediators Inflamm 2016;2016:8603164. doi:10.1155/2016/8603164.
15. Stirpe F, Ravaioli M, Battelli MG, et al. Xanthine oxidoreductase activity in human liver disease. Am J Gastroenterol 2002;97:2079–2085. doi:10.1111/j.1572-0241.2002.05925.x.
16. Wakabayashi Y, Fujita H, Morita I, et al. Conversion of xanthine dehydrogenase to xanthine oxidase in bovine carotid artery endothelial cells induced by activated neutrophils: involvement of adhesion molecules. Biochim Biophys Acta 1995;1265:103–109. doi:10.1016/0167-4889(94)00202-p.
17. Sumida Y, Niki E, Naito Y, et al. Involvement of free radicals and oxidative stress in NAFLD/NASH. Free Radical Res 2013;47:869–880. doi:10.3109/10715762.2013.837577.
18. McNally JS, Saxena A, Cai H, et al. Regulation of xanthine oxidoreductase protein expression by hydrogen peroxide and calcium. Arterioscler Thromb Vasc Biol 2005;25:1623–1628. doi:10.1161/01.ATV.0000170827.16296.6e.
19. Masarone M, Rosato V, Dallio M, et al. Role of oxidative stress in the pathophysiology of nonalcoholic fatty liver disease. Oxid Med Cell Longev 2018 ID 9547613. doi:10.1155/2018/9547613.
20. García-González V, Delgado-Coello B, Pérez-Torres A, et al. Reality of a vaccine in the prevention and treatment of atherosclerosis. Arch Med Res 2015;46:427–437. doi:10.1016/j.arcmed.2015.06.004.
21. Mas-Oliva J, Delgado-Coello B, Méndez-Acevedo K. Novel intranasal anti-CETP vaccine against the development of atherosclerosis and fatty liver disease. Atherosclerosis 2016;252:e238. doi:10.1016/j.atherosclerosis.2016.07.020.
22. Mas-Oliva J, Delgado-Coello B, Méndez-Acevedo KM, et al. Preclinical evidence studying intranasal HB-ATV-8 vaccines in a porcine model of atherosclerosis shows high efficiency in the prevention of atherogenesis and fatty liver disease. Atherosclerosis 2017;263:e52. doi:10.1016/j.atherosclerosis.2017.06.177.
23. Gutiérrez-Vidal R, Delgado-Coello B, Méndez-Acevedo KM, et al. Therapeutic intranasal vaccine HB-ATV-8 prevents atherogenesis and non-alcoholic fatty liver disease in a pig model of atherosclerosis. Arch Med Res 2018;49:456–470. doi:10.1016/j.arcmed.2019.01.007.
24. Brown GT, Kleiner DE. Histopathology of nonalcoholic fatty liver disease and nonalcoholic steatohepatitis. Metabolism 2016;65:1080–1086. doi:10.1016/j.metabol.2015.11.008.
25. Ramos de Andrade D Jr, Ramos de Andrade D, Alves do Santos S. Study of rat hepatocytes in primary culture submitted to hypoxia and reoxygenation: action of the cytoprotectors prostaglandin E1, superoxide dismutase, allopurinol and verapamil. Arq. Gastroenterol. 2009;46:333–340. doi:10.1590/S0004-2803200900040001.
26. Luo S, Levine RL. Methionine in proteins defends against oxidative stress. FASEB J 2009;23:464–472. doi:10.1096/fj.08-118414.
27. Black D, Lyman S, Qian T, et al. Transforming growth factor beta mediates hepatocyte apoptosis through Smad3 generation of reactive oxygen species. Biochimie 2007;89:1464–1473. doi:10.1016/j.biochi.2007.09.001.
28. Ye TJ, Lu YL, Yan XF, et al. High mobility group box-1 release from H2O2-injured hepatocytes due to sirt1 functional inhibition. World J Gastroenterol 2019;25:5434–5450 PMID: 31576091. doi:10.3748/wjg.v25.i36.5434.
29. Diamantino TC, Almeida E, Soares AM, Guilhermino L. Lactate dehydrogenase activity as an effect criterion in toxicity tests with Daphnia magnastraus. Chemosphere 2001;45:553–560. doi:10.1016/s0045-6535(01)00029-7.
30. Morelli A, Comeglio P, Filippi S, et al. Mechanism of action of phosphodiesterase type 5 inhibition in metabolic syndrome-associated prostate alterations: an experimental study in the rabbit. Prostate 2013;73:428–441. doi:10.1002/pros.22584.
31. Taylor E, Huang N, Bodde J, et al. MRI of atherosclerosis and fatty liver disease in cholesterol fed rabbits. J Transl Med 2018;215. doi:10.1186/s12967-018-1587-3.
32. Yang C, Yang S, Xu W, et al. Association between the hyperuricemia and nonalcoholic fatty liver disease risk in a Chinese population: A retrospective cohort study. PLoS One 2017:e0177249. doi:10.1371/journal.pone.0177249.
33. Nishikawa T, Nagata N, Shimakami T, et al. Xanthine oxidase inhibition attenuates insulin resistance and diet-induced steatohepatitis in mice. Sci Rep 2020;10:815. doi:10.1038/s41598-020-57784-3.
34. Lopez D. PCSK9: An enigmatic protease. Biochim Biophys Acta 2008;1781:184–191. doi:10.1016/j.bbalip.2008.01.003.
35. Lebeau P, Al-Hashimi A, Sood S, et al. Endoplasmic reticulum stress and Ca2+depletion differentially modulate the sterol regulatory protein PCSK9 to control lipid metabolism. J Biol Chem 2017;292:1510–1523. doi:10.1074/jbc.M116.744235.
36. Miyazaki T, Miyazaki A. Emerging roles of calpain proteolytic systems in macrophage cholesterol handling. Cell Mol Life Sci 2017;74:3011–3021. doi:10.1007/s00018-0172528-7.
37. Lippi G, Montagnana M, Franchini M, et al. The paradoxical relationship between serum uric acid and cardiovascular disease. Clin Chim Acta 2008;392:1–7. doi:10.1016/j.cca.2008.02.024.
38. Huang Q, Yu J, Zhang X, et al. Association of the serum uric acid level with liver histology in biopsy-proven non-alcoholic fatty liver disease. Biomed Rep 2016;1:188–192. doi:10.3892/br.2016.698.
39. Losenkova K, Zuccarini M, Helenius M, et al. Epithelial cells cope

with hypoxia-induced depletion of ATP via activation of cellular purine turnover and phosphotransfer networks. Biochim Biophys Acta - Molecular Basis of Disease 2018;1864:1804–1815. doi:10.1016/j.bbadis.2018.03.001.
40. Guérin P, El Mouatassim S, Ménézo Y. Oxidative stress and protection against reactive oxygen species in the pre-implantation embryo and its surroundings. Hum Repro Update 2001;7 175–18doi.org/. doi:10.1093/humupd/7.2.175.
41. Choi YJ, Shin HS, Choi H, et al. Uric acid induces fat accumulation via generation of endoplasmic reticulum stress and SREBP-1c activation in hepatocytes. Lab Invest 2014;94:1114–1125. doi:10.1038/labinvest.2014.98.
42. Taylor RS, Taylor RJ, Bayliss S, et al. Association Between Fibrosis Stage and Outcomes of Patients With Nonalcoholic Fatty Liver Disease: A Systematic Review and Meta-Analysis. Gastroenterology 2020;158:1611–1625 e12doi.org/. doi:10.1053/j.gastro.2020.01.043.
43. Bush KT, Wu W, Lun C, et al. The drug transporter OAT3 (SLC22A8) and endogenous metabolite communication via the gut-liver-kidney axis. J Biol Chem 2017;292:15789–15803. doi:10.1074/jbc.M117.796516.
44. Xu L, Shi Y, Zhuang S, et al. Recent advances on uric acid transporters. Oncotarget 2017;8:100852–100862. doi:10.18632/oncotarget.20135.
45. Maithili Karpaga Selvi N, Sridhar MG, Swaminathan RP, et al. Curcumin attenuates oxidative stress and activation of redox-sensitive kinases in high fructose-and high-fat-fed male Wistar rats. Sci Pharm 2015;83:159–175. doi:10.3797/scipharm.1408-16.
46. Alía M, Ramos S, Mateos R, et al. Response of the antioxidant defense system to terbutyl hydroperoxide and hydrogen peroxide in a human hepatoma cell line (HepG2). J Biochem Mol Toxicol 2005;19:119–128. doi:10.1002/jbt.20061.
47. Renaud HJ, Cui JY, Lu H, et al. Effect of diet on expression of genes involved in lipid metabolism, oxidative stress, and inflammation in mouse liver–insights into mechanisms of hepatic steatosis. PLoS One 2014;9:e88584. doi:10.1371/journal.pone.0088584.
48. Zhang Y, Cui Y, Wang X-L, et al. PPARα/γ agonists and antagonists differently affect hepatic lipid metabolism, oxidative stress and inflammatory cytokine production in steatohepatitic rats. Cytokine 2015;75:127–135. doi:10.1016/j.cyto.2015.05.031.
49. Damián-Zamacona S, Toledo-Ibelles P, Ibarra-Abundis MZ, et al. Early transcriptomic response to LDL and oxLDL in human vascular smooth muscle cells. PLoS One 2016;11:e0163924. doi:10.1371/journal.pone.0163924.
50. Jiménez-Corona AE, Damián-Zamacona S, Pérez-Torres A, et al. Osteopontin upregulation in atherogenesis is associated with cellular oxidative stress triggered by the activation of scavenger receptors. Arch Med Res 2012;43:102–111. doi:10.1016/j.arcmed.2012.03.001.